HHS Public Access

Author manuscript

Mucosal Immunol. Author manuscript; available in PMC 2017 December 15.

Published in final edited form as:

Mucosal Immunol. 2018 March ; 11(2): 345–356. doi:10.1038/mi.2017.52.

Tricellulin is regulated via interleukin 13 receptor α2, affects macromolecule uptake, and is decreased in ulcerative colitis

SM Krug[1], **C Bojarski**[2], **A Fromm**[1], **IM Lee**[1], **P Dames**[1], **JF Richter**[3], **JR Turner**[4], **M Fromm**[1,a], and **JD Schulzke**[1,a]

[1]Clinical Physiology, Department of Gastroenterology, Rheumatology and Infectious Diseases, Charité – Universitätsmedizin Berlin, Campus Benjamin Franklin, Berlin, Germany

[2]Department of Gastroenterology, Rheumatology and Infectious Diseases, Charité – Universitätsmedizin, Campus Benjamin Franklin, Berlin, Germany

[3]Institute for Anatomy II, Jena University Hospital, Jena, Germany

[4]Departments of Pathology and Medicine (GI), Brigham and Women's Hospital and Harvard Medical School, Boston, USA

Abstract

In the two inflammatory bowel diseases, ulcerative colitis (UC) and Crohn's disease (CD), altered expression of tight junction (TJ) proteins leads to an impaired epithelial barrier including increased uptake of luminal antigens supporting the inflammation. Here we focused on regulation of tricellulin, a protein of the tricellular TJ essential for the barrier against macromolecules, and hypothesized a role in paracellular antigen uptake. We report that tricellulin is downregulated in UC, but not in CD, and that its reduction increases the passage of macromolecules. Using a novel visualization method, passage sites were identified at TJ regions usually sealed by tricellulin. We show that interleukin-13 (IL-13), beyond its known effect on claudin-2, downregulates tricellulin expression. These two effects of IL-13 are regulated by different signaling pathways: The IL-13 receptor α1 upregulates claudin-2, while IL-13 receptor α2 downregulates tricellulin. We suggest to target the α2 receptor in future developments of therapeutical IL-13-based biologicals.

Corresponding author: Jörg-Dieter Schulzke, Address: Clinical Physiology, Department of Gastroenterology, Rheumatology and Infectious Diseases, Charité – Universitätsmedizin Berlin, Campus Benjamin Franklin, Hindenburgdamm 30, 12203 Berlin, Germany, joerg.schulzke@charite.de phone: +49 30 450-514531 fax: +49 30 450-514962.

[a]These authors contributed equally

Supplementary Material is linked to the online version of the paper at http://www.nature.com/mi

Author Contribution

Design of work: SMK, MF, JRT, JDS
Data aquiration: SMK, CB, AF, IML. PD
Result interpretation: SMK, JFR, JRT,MF, JDS
Drafting of manuscript: SMK, MF
Revision of manuscript: CB, AF, IML, PD, JFR, JRT, MF, JDS
Appoval of final version: SMK, CB, AF, IML, PD, JFR, MF, JDS

Disclosure

All authors have no conflicts to declare.

Introduction

The intestinal epithelium consists of a polarized single cell layer with a multi-protein complex, the tight junction (TJ) which strictly regulates paracellular passage of ions, molecules and water. This regulation is determined by transmembrane proteins of the TJ comprising of four families: four-transmembrane TJ proteins include the family of claudins with 2-members in mammals(1), and the tight junction-associated MARVEL proteins (TAMP)(2) containing occludin(3), MARVEL D3(2, 4) and tricellulin(5). Most of the claudins form barriers but some form paracellular ion and water channels(6, 7). Junctional adhesion molecules (JAM(8)) and the most recently described group of angulins(9) span the membrane once. Angulins and tricellulin are located at the tricellular TJ (tTJ), the region where three or more cells meet and their bicellular TJ (bTJ) converge laterally forming a central tube. We have previously shown that tricellulin plays an important role in sealing the tTJ, particularly to macromolecules(10, 11).

Integrity of the epithelial barrier is impaired in a variety of pathological conditions, for example in the inflammatory bowel diseases (IBD) Crohn's disease (CD)(12) and ulcerative colitis (UC)(13). Although pathogenesis of the barrier defect in IBDs is still unclear(14), several studies demonstrate that pro-inflammatory cytokines including TNFα(15), IFNγ(16, 17) and interleukin-13 (IL-13)(18, 19) alter barrier function by changing TJ protein function and expression. For example, IL-13 has been linked as proinflammatory cytokine to UC, stimulating epithelial cell apoptosis and enhancing barrier defects, predominantly by upregulation of the cation-selective paracellular channel claudin-2(18–20).

IL-13 is a cytokine which is released by Th2 cells sharing biological properties with IL-4 and both cytokines are involved in immune-mediated processes, where they often act in an manner that opposes Th1-polarized inflammation(21). Not only in UC but also in asthma IL-13 and IL-4 have been reported to work synergistically to enhance inflammatory activity. Two IL-13 receptor complexes are described and the balance between these is believed to regulate both quantitative and qualitative effects of IL-13 signaling(22–25). The first consists of a receptor complex composed of the IL-4 receptor α (IL4Rα) and the IL-13 receptor α1 (IL13Rα1)(26, 27), the second is generated by IL-13 receptor α2 (IL13Rα2).

For IL4Rα/IL-13Rα1 signaling, phosphorylation of STAT1(28), STAT6(29), and STAT3(28) have been reported as well as signaling via the MAPK and PI3K pathways(30–32) and have been connected to claudin-2 upregulation by IL-13(33).

Two variants of IL13Rα2 which differ in activity have been described, a soluble and a cell surface-bound. The soluble form found in urine and serum of mice(34) is described as a decoy receptor that partially inhibits effects of IL-13(23, 35); function of the human soluble form is more controversial(36, 37). In contrast, the cell surface-bound form of IL13Rα2 stimulates the transcription factor complex activator protein (AP-1)(38, 39), phosphorylates STAT3(40), and enhances MAPK(38), PI3K(41) and ERK1/2 signaling(39), both in rodents and humans.

In this study, we analyzed the expression of the TJ protein tricellulin (Tric) in IBD and found it to be downregulated in UC, but not CD. We showed that this altered expression is driven

by the UC key cytokine IL-13 via IL13Rα2. While IL-13 also upregulates claudin-2 expression, we found that the signaling mechanisms differed from those responsible for tricellulin downregulation. In contrast to increased water and cation flux after claudin-2 upregulation, we found that IL-13-induced suppression of tricellulin led to enhanced paracellular macromolecular uptake which we were able to localize at tTJs. This may represent a novel mechanism for increased luminal uptake of antigens in UC.

Results

When comparing membrane protein expression levels of tricellulin within sigmoid colon tissue of IBD and control (Ctrl) patients, it was conspicuous that there was profound and substantial reduction of tricellulin (Tric) in UC, but not in CD patients (Fig. 1A+D), comparable to changes reported for claudin-4 (Cldn-4) (42) (Fig. 1C+D). This finding is also in line with GEO expression data, reporting tricellulin (synonym: MARVEL D2) to be downregulated in inflamed UC tissue (GDS3119)(43, 44), but not in CD (GDS560)(45). Claudin-2 (Cldn-2) nearly absent in Ctrl served as control for changes in IBD(46) (Fig. 1B +D). Impedance spectroscopic analysis of UC samples revealed that, although transepithelial resistance (TER) was similar to that of controls, epithelial resistance was decreased, while subepithelial resistance was increased due to inflammatory thickening of the subepithelium due to edema and condensed collagenous fibers (Fig. 1E). Permeabilities for paracellular flux markers as fluorescein and 4 kDa-FITC-dextran (FD4) were increased indicating an impaired paracellular barrier (Fig. 1F). Immunostainings of cryosections (Fig. 2) revealed that in control patients, tricellulin was present all along the crypt and the surface epithelium, while claudin-2 was only detectable in the depths of the crypts. In both IBD, claudin-2 expression was increased and localization was extended to the total length of the crypts and to the surface epithelium. Tricellulin was decreased in UC patients, while in CD patients a shift of localization seemed to occur. While in the crypts the signal seemed to be slightly reduced, an increase of signals was observed in the surface epithelium, which also was extended from the apicolateral regions of the TJ to more basolateral regions. However, these changes in localization did not occur in all CD samples analyzed.

To investigate the origin of the UC-specific change in tricellulin expression, the intestinal epithelial cell line HT-29/B6 was treated with cytokines known to be involved in IBD (Fig. S1). IL-13, a major effector in UC (18), not only increased claudin-2 but also decreased tricellulin expression (Fig. 3A, S1). All other cytokines tested affected only claudin-2 (Fig. S1). On mRNA level, tricellulin was reduced to 64±8% (**$p<0.01$, n=6) and claudin-2 increased to 238±24% of controls (***$p<0.001$, n=6). mRNA and protein half-lives were not affected, indicating that IL-13 did not affect protein or mRNA stability. At 100 ng/ml, IL-13 had no effect on epithelial apoptotic rate (Tab. S1), measured by TUNEL staining and previously reported (47).

IL-13 decreased TER by 62%, while permeability for the macromolecule FD4 was increased from 0.06±0.01 to $0.15\pm0.01\cdot10^{76}$ cm/s (Fig. 3B+C, n=7, ***$p<0.001$). Comparable results were achieved when tricellulin was downregulated by stable transfection with specific shRNA (Fig. 3D+E), namely increased permeability to FD4 (n=11) and to 10 kDa-FITC dextran (n=4; Fig. 3F, Fig. S2). This provides direct evidence that the observed increase in

macromolecule permeability, i.e. the leak pathway (48), was based on the decrease tricellulin alone, not on alterations of claudin-2 or of occludin, since expression of both was unchanged (Fig. 3D+E). Neither was the expression of angulins affected by tricellulin knockdown (Fig. S3). Together with this, a decrease in TER occurred (Vec: 1325±174 Ω·cm^2; shTRIC: 730±64 Ω·cm^2; *p<0.05, n=11) which, however, was lower as in the IL-13-treated cells because the TER-decreasing effect of claudin-2 was lacking here.

To confirm the cell culture findings for IL-13 and tricellulin in colon epithelium, mice were treated with IL-13 and protein expression of tricellulin as well as functional consequences for the intestine were analyzed by electrophysiological experiments. The chosen dose and duration of the treatment did not lead to obvious changes in the intestinal architecture (Fig. S4A), but a decrease in epithelial resistance was observed indicating impairment of the mucosal barrier, while the subepithelial resistance was unaffected (Fig. S4B, *p<0.05, n=5). Macromolecular permeability for FD4 was doubled in the colon of IL-13-treated mice (Fig. 4A, *p<0.05, n=8). Also, the effect of IL-13 on expression and localization of tricellulin as well as of claudin-2 was reproducible in mice (Fig. 4B+C, *p<0.05, n=7–9; Fig. S4C).

To elucidate the signaling of IL-13 involved in tricellulin downregulation several approaches were tested in cell culture. 1 h pretreatment with inhibitory antibodies against the two IL-13 receptors was used to inhibit the interaction of IL-13 (Fig. 5). Importantly, anti-IL13Rα1 was able to block the increase in claudin-2 expression, but not the decrease of tricellulin. In contrast, anti-IL13Rα2 inhibited the decrease of tricellulin, but not the claudin-2 effect (Fig. 5A+B). When analyzing the effect on macromolecule permeability using FD4, the inhibition of IL13Rα1 by the inhibitory antibody had no suppressing effect on the increase of FD4 permeability after treatment with IL-13. When interaction of IL-13 with the IL13Rα2 was inhibited, permeability for FD4 was comparable to untreated cells (Fig. 5C).

Also treatment of STAT6$^{-/-}$ mice with IL-13 reduced tricellulin expression, indicating that STAT6 and upstream IL13Rα1 signaling were not involved (Fig. 7A+B). In contrast, claudin-2 expression was not increased in intestinal mucosae from IL-13-treated STAT6$^{-/-}$ mice, providing strong data that support for the conclusion from *in vitro* data(33) that IL13Rα-induced STAT6 activation regulates claudin-2 expression. These differences implicate the IL13Rα2 signaling pathway, which is independent of STAT6, to operate in tricellulin downregulation. Consistent with this, IL-13 in T84 cells, which do not express IL13Rα2 (Fig. S5C), upregulated claudin-2 expression but did not downregulate tricellulin (Fig. S5A+B). The same was observed when IL13Rα2 was downregulated by stable transfection with specific shRNA (Fig. 6A–D). The knockdown of IL13Rα2 also abolished the macromolecule permeability increase in response to IL-13 (Fig. 6E), supporting the finding of tricellulin downregulation to be involved in this permeability increase.

To analyze the signal transduction pathway in more detail, several inhibitors known to be regulated by IL-13(28–33, 38–41) were added before treating the cells with IL-13. For this, protein (Fig. 7C+Fig. S6A) as well as mRNA (Fig. S6B) levels were analyzed. Claudin-2 upregulation was blocked when IL13Rα1-related pathways were inhibited by AS151–499, SAHA (both affecting STAT6), LY294002 (PI3K) or U0126 (MAPK), confirming the findings from the inhibitory antibodies and STAT6$^{-/-}$ mice. In contrast, downregulation of

tricellulin was inhibited when IL13Rα2 pathways were targeted with JNK V, (JNK), U0126 (MAPK, ERK1/2), or Tanshinone IIa (AP-1). However, not all drugs targeting IL13Rα2 signaling prevented tricellulin downregulation, for example PI3K. Conversely, JAK1/2 inhibition using baricitinib and JAK3 inhibition using JAK3-inhibitor II had no effect on claudin-2 expression, although each is thought to be involved in signaling by the IL4Rα/IL13Rα1 complex. The data indicate, however, that JAK1 and/or JAK2 are involved in tricellulin regulation.

To further delineate signaling, expression and phosphorylation of potential IL13Rα2 signaling intermediates were analyzed. To exclude effects being non-specific for tricellulin, the inhibitor U0126, which was shown to block the tricellulin downregulation and which is supposed to be involved early in the signaling, was used for comparison (Fig. 7D). c-Fos was highly upregulated by IL-13, an effect which was blockable by U0126. All other effects on total protein expression were either not significant or only slightly attenuated by U0126 (Fig. 7E). When comparing the phosphorylation status of the respective proteins (Fig. 7F), it became obvious that c-Fos phosphorylation was not affected by U0126. However, IL-13 alone markedly decreased c-Fos phosphorylation and increased its total expression. For several other intermediates phosphorylation ratios were increased during IL-13-induced tricellulin downregulation; IL-13 increased phosphorylation of FRA-1 and of p44/42, an effect that was inhibited when U0126 was present. Interestingly, IL-13 reduced c-jun phosphorylation at S63, and this effect was also inhibited by U0126. Effects of IL-13 on p38 MAPK and p54 SAPK phosphorylation were not inhibited by U0126 and may therefore be unrelated to tricellulin downregulation.

Tricellulin has been reported as barrier-forming TJ protein inhibiting excessive macromolecule passage through the tTJ (10, 11). As IL-13 treatment lead to increased FD4 and FD10 permeability, we investigated the site of macromolecule passage through the bTJ and the tTJ of HT-29/B6 monolayers using the recently developed sandwich assay(49). In controls, i.e. when high amounts of tricellulin are present, no permeation of biotin-labelled-TRITC-dextran 10 kDa was observed (Fig. 8, upper panel, A and B). In contrast, in IL-13-treated cells tricellulin was reduced and apically added 10 kDa dextran appeared on the basolateral side (Fig. 8, lower panel, A and B). In a merged view (Fig. 8, lower panel, D), the passage site appeared preferentially at tricellular TJs, in rare cases also at TJs where four cells meet.

When the cells were additionally incubated with the inhibitor Tanshinone IIa, this passage was strongly diminished (Fig. S7), an effect that we also observed in global analysis of macromolecule permeability performing flux measurements in Ussing chambers (Fig. S8). IL-4 targeting the complex formed by IL13Rα1 and IL4R (Fig. 9) had an effect only on claudin-2 but not on tricellulin expression (Fig. S1). Consistently, we observed no increased passage of the biotin-labelled-TRITC-dextran 10 kDa under these conditions (Fig. S6).

In order to demonstrate the localization site of macromolecule passage, representative Z-stack images were rendered into three-dimensional movies (Supplementary movie M1). Comparable observations were made using the shTRIC clone (Fig. S7 and Supplementary

movie M2), supporting that the macromolecule passage may depend on the level of tricellulin present in tTJs.

Discussion

Tricellulin is downregulated in UC, but not in CD

In this study we analyzed the expression of the tricellular TJ (tTJ) protein tricellulin in CD and UC. Though the intestinal barrier is impaired in both CD and UC, we find tricellulin to be downregulated only in UC, indicating UC specific down-regulation, but not in CD. However, the predominant localization of tricellulin was shifted towards the surface epithelium in CD, which might indicate that changes in proteins that regulate the correct localization of tricellulin occur in CD. For example, LSR is known to be predominantly localized within the depths of the crypts, while ILDR-1 can be found along the whole crypt(9). Thus, regulation of tricellulin depends also on other tTJ proteins and might be complex in CD, even if total expression remained unchanged. Elucidation of this regulation and involvement of other components of the tTJ in CD need to be studied in detail and will be object of further examination.

IL 13 leads to increased paracellular passage of macromolecules via tricellulin downregulation

In human biopsies as well as in mice and in HT-29/B6 monolayers, IL-13-induced tricellulin downregulation resulted in increased macromolecule permeability. Obtaining independent evidence, targeted tricellulin knockdown had the same effect on macromolecule passage, which is not dependent on occludin or claudin-2 because both were unchanged. These findings were consistent with previous results from our and other labs(5, 10, 11, 50). Our results were corroborated by three-dimensional visualization of macromolecules passing IL-13-treated HT-29/B6 cells predominantly at sites where more than two cells meet.

Taken together, our data demonstrate that the IL-13-induced permeability increase for macromolecules is directly linked to tricellulin. The mechanistic relation between tricellulin and opening the passage site for macromolecules is unknown yet and will be the target of future studies.

In conclusion, tricellulin and the tTJ are critical to maintenance of the paracellular barrier to macromolecular flux in the intestine. In early stages of UC, tricellulin downregulation therefore might already destabilize tricellular and TJ tightness, thereby allowing passage of antigens that may further promote the inflammatory process.

IL 13 regulates claudin 2 and tricellulin via different signaling pathways

To elucidate the regulation beyond the decreased tricellulin expression in UC, we concentrated on IL-13, which is a key cytokine in UC(18). Treatment with IL-13 increased claudin-2 as described earlier(18–20) and we show here that it also decreased tricellulin expression. This effect was demonstrated in cell cultures as well as in mice treated with IL-13.

After analyzing the influence of blocking antibodies, knockdown of IL13Rα2, inhibitors of reported signaling pathways and mice lacking STAT6, we found that two pathways are involved and that each had distinct effects. Based on the established signaling cascades of IL-13 (22–29) we conclude that (Fig. 9) (i) claudin-2 expression and trans-tight junction pore pathway flux are upregulated via IL-13 binding to the IL4Rα/IL13Rα1 complex and the subsequent activation of STAT6, PI3K and MAPK. (ii) Tricellulin is downregulated and trans-tight junction leak pathway flux is enhanced via IL-13 binding to IL13Rα2. The subsequent signaling involved ERK1/2, JNK and AP-1.

The transcription factor AP-1 may be composed of dimers of proteins belonging to the family of Fos, Jun or ATF proteins. Analysis of the most common AP-1 sub-proteins revealed that in tricellulin downregulation by IL-13, higher expression levels of c-Fos as well as the phosphorylation status of FRA-1 and c-jun (position S63) are involved as inhibition by U0126 affected these alterations as well as the tricellulin decrease.

Taken together, IL-13 affects both, the bTJ and the tTJ. Claudin-2 as size-restrictive channel for small cations and water is a main factor in enhancing the high-capacitive pore-pathway, as by upregulation of claudin-2 permeability for Na^+ increases. This can also be retraced by TER decrease, as TER depends on ions.

The further influence of IL-13 on the tTJ via downregulation of tricellulin affects the leak pathway as permeability for macromolecular solutes is increased. However, as in tight epithelia the occurrence of bicellular conductive channels is low (tight epithelia possess a lower paracellular than transcellular conductance), opening of the tTJ also affects ion permeability.

Thus, both effects of IL-13 need to be taken in account when developing new strategies of intervention.

Demand of new receptor specific IL 13 based intervention strategies

Our findings indicate that the increased macromolecule passage in UC is at least partly caused by tricellulin downregulation and that, among all cytokines tested in HT-29/B6 cells, only IL-13 causes tricellulin downregulation. In contrast, claudin-2 expression can be upregulated by several cytokines involved in IBD. The role of claudin-2 in IBD has been linked to leak flux diarrhea as claudin-2 increases permeability for small cations as well as for water. On the other hand, recent studies on claudin-2-overexpressing mice suggested that claudin-2 also may have protective properties, as these mice were protected against DSS-induced colitis. Besides feasible dilution of the DSS by enhanced paracellular water flux by claudin-2, it might be speculated whether the additionally described lower immune activation and increased colonocyte proliferation in these mice were leading to the protection(51). Increase of claudin-2 and water flux in IBD might in conclusion have two effects, it may contribute to leak-flux diarrhea and by this may serve as a beneficial rinsing of the inflamed mucosa (“enteric tears”(52)).

IL-13 had been proposed as key player in both UC and asthma, and great hope has been linked to development of IL-13-focused biologics. However, to date, all approaches have

failed: (i) Anrukinzumab, an antibody blocking the attachment of IL-13 to IL4Rα by binding to IL-13, showed no significant therapeutic effect in active UC(53), which is not surprising on the basis of our present data, since the binding to IL13Rα2 was unaffected. (ii) A second antibody, tralokinumab which binds and neutralizes IL-13, induced no clinical improvement in UC but at least led to higher clinical remission rates in a subset of patients(54). (iii) A third antibody, GSK69586, was directed against the IL-13 binding to both receptors, but was only tested in asthma patients so far (55, 56).

We hypothesize that the earlier attempts to develop biologics targeting IL-13 have failed because they did not differentiate between the two pathways. Targeting solely the IL-13 receptor α1 might be less beneficial or even harmful, because blocking the UC-induced claudin-2 increase hinders the beneficial rinsing of the inflamed mucosa. In contrast, targeting the IL-13 receptor α2, however, would block the UC-induced decrease of tricellulin and by this would restore the barrier against the uptake of inflammatory macromolecules. We suggest that inhibiting the IL-13 receptor α2 pathway may be effective in UC, maybe most effective in early stages or in an attempt to achieve remission, when after healing of gross lesions this macromolecule leak is functionally essential. Therefore new approaches differentiating the two receptors are required for successful treatment.

Not less importantly, tricellulin itself might be another potential candidate for intervention, targeting the loss of the macromolecular barrier and at the same time uncontrolled luminal uptake of macromolecular agents, especially in early disease states before gross lesions develop.

Methods

Patients and Tissue Preparation

Biopsies from sigmoid colon were obtained from patients with histologically confirmed active ulcerative colitis (UC, n=20, median age of 34 years, range 20–79 years; 9 female and 11 male) or Crohn's disease (CD, n=17, median age of 38 years, range 21–63 years; 9 female and 8 male) and from 21 control subjects (Ctrl, median age of 50 years, range 19–75 years; 14 female and 7 male). 17 UC patients received prednisolone (median dose 15 mg/day, range 5–70 mg/day). Of these, 9 patients also received 5-aminosalicylic acid (1.5–5 g/day). 3 UC patients only received 5-aminosalicylic acid. Measurements were performed on inflamed specimens without visible erosions/ulcers (histologically mild to moderate inflammation, e.g. Fig. S9). The specimens were spread and glued with histoacryl tissue glue (B Braun, Melsungen, Germany) to a support disk and mounted in Ussing-type chambers with an exposed tissue area of 0.49 cm^2. The study design was approved by the local ethics committee (EA4/015/13).

Cell culture and transfections

The human colon cell line HT-29/B6 exhibits a transepithelial resistance and other basic properties making it an excellent model of colonic epithelia(57). For stable tricellulin knockdown, HT-29/B6 cells were transfected with pLKO.1-puro vector containing a sequence for shRNA targeting tricellulin (TRCN00000-2636NM_144-24.1-988s1c1TRC 1,

Sigma-Aldrich) or targeting IL13Rα2 (TRCN0000058526_SHCLNG-NM_000640, Sigma-Aldrich) using *Amaxa*™ Nucleofector™ Technology. Puromycin-resistant clones were screened for knockdown by western blot. For experimentation, cell monolayers were grown on Millicell-PCF inserts (pore size 3.0 μm, effective area 0.6 cm^2, Millipore, Bedford, MA). Confluent cell layers exhibiting transepithelial resistances (TER) above 600 $\Omega \cdot cm^2$ were used 7 days after seeding.

Cytokine and inhibitor experiments

Cells were incubated as listed in table 1 for 24 h (TNFα) or 48 h (all others). Treatment with inhibitors occurred 1 h before IL-13 application. For experiments with inhibitory antibodies, cells were pretreated for 1 h with 5 μg/mL mouse anti-CD213a1/IL13Ra1 (AM31180AF-N, Acris, Herford, Germany) or mouse anti-IL13Ra2 (clone 2E10, Sigma-Aldrich) before addition of IL-13.

Treatment of mice with IL 13

BALB/c wild type mice (Charité, Forschungseinrichtungen für experimentelle Medizin, Berlin, Germany) and $STAT6^{-/-}$ mice (Jackson Laboratory, Bar Harbor, USA) were housed, fed and handled under accordance with the rules of institutional animal care. Experiments were approved by the Landesamt für Gesundheit und Soziales Berlin (G 0208/12). 12 – 20 weeks-old female mice were injected intraperitoneally with 3 μg murine IL-13 (BioLegend GmbH, Fell, Germany) diluted in 300 μl PBS with 0.1% BSA or vehicle alone daily for three days. 72 h after the last treatment, mice were sacrificed and colonic tissue was collected for further analysis.

Immunofluorescent staining

Human biopsies and mouse tissue was cryosectioned and fixed with methanol (−20 °C). After permeabilization with 0.5% Triton-X100 and blocking with 5% goat serum, sections were incubated with primary antibodies against claudin-2 (Invitrogen, Karlsruhe, Germany; 1:200) and tricellulin (Abfinity, Invitrogen; 1:600), followed by washing steps and incubation with the respective secondary antibodies (Alexa Fluor 488 goat anti-mouse and Alexa Fluor 594 goat anti-rabbit, each 1:500; Molecular Probes MoBiTec) and DAPI (1:1000). Images were obtained with a confocal laser scanning microscope (LSM 580, Zeiss).

Electrophysiological and flux measurements

Electrophysiological and flux studies were performed in Ussing chambers under short-circuit conditions as described earlier.(46) For flux measurements, after apical addition of fluorescein (0.1 mM) or FITC-labeled and dialyzed 4 or 10 kDa dextran (0.4 mM, TdB Consultancy, Sweden) together with basolateral addition of unlabeled dextran of the same size (0.4 mM, Serva, Heidelberg, Germany), basolateral samples were taken at 0, 30, 60, 90, and 120 min. Tracer fluxes and apparent permeabilities were calculated from the amount of FITC-dextran in the basolateral compartment measured fluorometrically (Tecan Infinite M200, Tecan, Switzerland). One-path impedance analysis was performed employing specialized Ussing chambers as described.(58).

Western blotting, phosphorylation assays and protein stability

Cells were washed with ice-cold PBS, scraped from the permeable supports and incubated on ice in lysis buffer containing 10 mM Tris-Cl (pH 7.5), 150 mM NaCl, 0.5% (v/v) Triton X-100, 0.1% (w/v) SDS and protease inhibitors (Complete, Roche). Protein was obtained in the supernatant after a centrifugation at 15.000×g (15 min, 4°C).

For phosphorylation assays, cells were lysed at one hour after IL-13 treatment using phospholyis buffer (20 mM Tris-Cl (pH 7.5), 150 mM NaCl, 1 mM EDTA, 1 mM EGTA, 1% Trition X-100, 2.5 mM $Na_4P_2O_7$, 1 mM β-glycerophosphate, 1 mM Na_3VO_4, 1μg/mL leupeptin, 1mM PMSF).

For tissues, samples were homogenized in ice-cold lysis buffer (1 M Tris-Cl pH 7,4, 1 M $MgCl_2$, 0.5 M EDTA, 0.5 M EGTA, protease inhibitors) and pushed through a 1 mL hypodermic syringe with a 0.45 × 10 mm needle. Supernatants of a short centrifugation (1,000 ×g, 5 min, 4°C) were centrifuged (42,100 ×g, 30 min, 4°C) and the resulting pellets containing the membrane protein fraction were resolved in lysis buffer.

10 μg of the protein samples were electrophoresed on a SDS-polyacrylamide gel and then transferred to a PVDF membrane (Perkin Elmer). Proteins were detected by immunoblotting employing primary antibodies against claudin-2 and -4 (Invitrogen, Karlsruhe, Germany), tricellulin (Abfinity, Invitrogen), c-Fos, phopsho-c-Fos, c-jun, phosphor-c-junS63, phosphor-c-junS-3, FRA-1, phosphor-FRA1, SAPK/JNK, phosphor-SAPK/JNK, ERK1/2, phosphor-ERK1/2, p38 and phosphor-p38 (Cell Signaling Technology). For chemiluminescence detection, membranes were washed and incubated with Lumi-Light^{plus} (Roche). Specific signals were quantified by luminescence imaging (Fusion FX7, Vilber Lourmat, Eberhardzell, Germany) and quantification software (Multi Gauge V2.3, FujiFilm, Japan).

For analysis of protein stability, HT-29/B6 cells were cultured in the presence or absence of IL-13, while protein synthesis was blocked by addition of 100 μg/ml cycloheximide (Sigma-Aldrich) 2 h prior to cytokine treatment. Protein was isolated 0, 2, 8, 12, 24, 30 and 48 h after IL-13 addition, and tricellulin protein expression was evaluated by western blotting. Amounts of tricellulin were plotted against time on a logarithmic scale. The half-life ($T_{1/2}$) of the protein was calculated from the slope of the linear smoothing function.

Isolation of RNA, reverse transcription, qRT PCR and mRNA stability

RNA was isolated using the peqGOLD RNAPure (peqLab Biotechnologie GmbH, Erlangen, Germany) according to the manufacturer's instructions and RNA was quantified by NanoDrop® ND-1000 UV-Vis Spectrophotometer (peqLab Biotechnologie GmbH).

2 μg of total RNA per reaction were reverse-transcribed using High Capacity cDNA Reverse Transcription Kit (Applied Biosystems, Mannheim, Germany). Quantitative RT-PCR of tricellulin (Hs00930631_m1), claudin-2 (Hs00252666_s1) and GAPDH as control were amplified using taqman probes (Applied Biosystems). Differential expression was calculated according to the $2^{-\Delta\Delta CT}$ method.

For analysis of mRNA stability, HT-29/B6 cells were cultured in the presence or absence of IL-13, while RNA transcription 1 h in advance was blocked by addition of 7 μg/mL actinomycin D (Sigma-Aldrich). RNA was isolated 0, 6, 12, 24, and 28 h after actinomycin D addition, reversely transcribed, and quantified by RT-PCR. Amounts of the target-specific copies were plotted against time on a logarithmic scale and the half-life ($T_{1/2}$) of mRNA was calculated.

TUNEL staining

Cells were fixed in 1% paraformaldehyde and DNA was stained with a TUNEL assay (TdT-mediated X-dUTP nick end labeling; Roche, Mannheim, Germany). Labeled nuclei were counted and expressed as a fraction of total DAPI-stained nuclei.

Passage visualization

For visualization of macromolecule passage, the recently developed sandwich assay(49) was slightly modified. In brief, filter supports (pore size 0.45 μm) were transferred to chilled HEPES-buffered ringer, kept at 4 °C and basally incubated with 15 μM avidin (Lee Biosolutions) for 20 min. Excess avidin was removed by washing. 10 μM biotin-labelled TMR-dextran 10 kDa (Invitrogen) was added apically for 1 h and then carefully removed by washing. Cells were fixed with 2% paraformaldehyde (Electron Microscopy Sciences) and used for subsequent immunofluorescent staining of ZO-1 (BD, Heidelberg, Germany) and tricellulin (Abfinity, Invitrogen).

Statistical analysis

If not differently stated, data are expressed as mean values ± standard error of the mean (SEM) indicating n as the number of single, independent measurements. Statistical analysis was performed using Student's t-test with Bonferroni-Holm adjustment for multiple testing or the Mann-Whitney-test for not normally distributed data. $p<0.05$ was considered significant (*$p<0.05$, **$p<0.01$, ***$p<0.001$).

Supplementary Material

Refer to Web version on PubMed Central for supplementary material.

Acknowledgments

This study was supported by grants from the Deutsche Forschungsgemeinschaft (DFG FOR 721/2, KR 3807/171, Schu 559/11-2), from the Sonnenfeld-Stiftung Berlin, and from the US National Institutes of Health (DK061931).

Abbreviations

AP-1	activator protein 1
bTJ	bicellular tight junction
CD	Crohn's disease
Cldn	claudin

ERK1/2	extracellular-signal-regulated kinases 1 and 2
FeNO	exhaled nitric oxide
FD10	FITC-dextran 10 kDa
FD4	FITC-dextran 4 kDa
FITC	fluorescein isothiocyanate
IBD	inflammatory bowel disease
IL-13	interleukin-13
IL-4	interleukin-4
IL13Rα	IL-13 receptor alpha
IL4R	IL-4 receptor
INFγ	interferon gamma
JAK	Janus kinase
JAM	junctional adhesion molecule
JNK	c-Jun N-terminal kinase
MAPK	mitogen-activated protein kinases
MARVEL	MAL and related proteins for vesicle trafficking and membrane link
PI3K	phosphatidylinositide 3-kinase
R^{epi}	epithelial resistance
R^{sub}	subepithelial resistance
R^{t}	transepithelial resistance (R^{t}=TER=R^{epi}+R^{sub})
SAHA	suberoylanilide hydroxamic acid
SAPK	stress-activated kinase
STAT	signal transducers and activators of transcription
TAMP	tight junction-associated MARVEL proteins
TER	transepithelial resistance
TGFβ	transforming growth factor beta
TJ	tight junction
TNFα	tumor necrosis factor alpha
Tric	tricellulin

tTJ	tricellular tight junction
UC	ulcerative colitis

References

1. Mineta K, Yamamoto Y, Yamazaki Y, Tanaka H, Tada Y, Saito K, et al. Predicted expansion of the claudin multigene family. FEBS Lett. 2011; 585(4):606–12. [PubMed: 21276448]
2. Raleigh DR, Marchiando AM, Zhang Y, Shen L, Sasaki H, Wang Y, et al. Tight junction-associated MARVEL proteins marveld3, tricellulin, and occludin have distinct but overlapping functions. Mol Biol Cell. 2010; 21(7):1200–13. [PubMed: 20164257]
3. Furuse M, Hirase T, Itoh M, Nagafuchi A, Yonemura S, Tsukita S, et al. Occludin: a novel integral membrane protein localizing at tight junctions. The Journal of cell biology. 1993; 123(6 Pt 2):1777–88. [PubMed: 8276896]
4. Steed E, Rodrigues NT, Balda MS, Matter K. Identification of MarvelD3 as a tight junction-associated transmembrane protein of the occludin family. BMC Cell Biol. 2009; 10:95. [PubMed: 20028514]
5. Ikenouchi J, Furuse M, Furuse K, Sasaki H, Tsukita S, Tsukita S. Tricellulin constitutes a novel barrier at tricellular contacts of epithelial cells. J Cell Biol. 2005; 171(6):939–45. [PubMed: 16365161]
6. Colegio OR, Van Itallie CM, McCrea HJ, Rahner C, Anderson JM. Claudins create charge-selective channels in the paracellular pathway between epithelial cells. Am J Physiol Cell Physiol. 2002; 283(1):C142–7. [PubMed: 12055082]
7. Krug SM, Schulzke JD, Fromm M. Tight junction, selective permeability, and related diseases. Semin Cell Dev Biol. 2014; 36:166–76. [PubMed: 25220018]
8. Ebnet K, Suzuki A, Ohno S, Vestweber D. Junctional adhesion molecules (JAMs): more molecules with dual functions? J Cell Sci. 2004; 117(Pt 1):19–29. [PubMed: 14657270]
9. Higashi T, Tokuda S, Kitajiri S, Masuda S, Nakamura H, Oda Y, et al. Analysis of the 'angulin' proteins LSR, ILDR1 and ILDR2--tricellulin recruitment, epithelial barrier function and implication in deafness pathogenesis. J Cell Sci. 2013; 126(Pt 4):966–77. [PubMed: 23239027]
10. Krug SM, Amasheh M, Dittmann I, Christoffel I, Fromm M, Amasheh S. Sodium caprate as an enhancer of macromolecule permeation across tricellular tight junctions of intestinal cells. Biomaterials. 2013; 34(1):275–82. [PubMed: 23069717]
11. Krug SM, Amasheh S, Richter JF, Milatz S, Günzel D, Westphal JK, et al. Tricellulin forms a barrier to macromolecules in tricellular tight junctions without affecting ion permeability. Mol Biol Cell. 2009; 20(16):3713–24. [PubMed: 19535456]
12. Baumgart DC, Sandborn WJ. Crohn's disease. Lancet (London, England). 2012; 380(9853):1590–605.
13. Ordas I, Eckmann L, Talamini M, Baumgart DC, Sandborn WJ. Ulcerative colitis. Lancet (London, England). 2012; 380(9853):1606–19.
14. Scharl M, Rogler G. Inflammatory bowel disease pathogenesis: what is new? Current opinion in gastroenterology. 2012; 28(4):301–9. [PubMed: 22573190]
15. Chen P, Li J, Barnes J, Kokkonen GC, Lee JC, Liu Y. Restraint of proinflammatory cytokine biosynthesis by mitogen-activated protein kinase phosphatase-1 in lipopolysaccharide-stimulated macrophages. Journal of immunology (Baltimore, Md: 1950). 2002; 169(11):6408–16.
16. Bruewer M, Luegering A, Kucharzik T, Parkos CA, Madara JL, Hopkins AM, et al. Proinflammatory cytokines disrupt epithelial barrier function by apoptosis-independent mechanisms. Journal of immunology (Baltimore, Md: 1950). 2003; 171(11):6164–72.
17. Wang F, Graham WV, Wang Y, Witkowski ED, Schwarz BT, Turner JR. Interferon-gamma and tumor necrosis factor-alpha synergize to induce intestinal epithelial barrier dysfunction by up-regulating myosin light chain kinase expression. The American journal of pathology. 2005; 166(2): 409–19. [PubMed: 15681825]

18. Heller F, Florian P, Bojarski C, Richter J, Christ M, Hillenbrand B, et al. Interleukin-13 is the key effector Th2 cytokine in ulcerative colitis that affects epithelial tight junctions, apoptosis, and cell restitution. Gastroenterology. 2005; 129(2):550–64. [PubMed: 16083712]
19. Weber CR, Raleigh DR, Su L, Shen L, Sullivan EA, Wang Y, et al. Epithelial myosin light chain kinase activation induces mucosal interleukin-13 expression to alter tight junction ion selectivity. J Biol Chem. 2010; 285(16):12037–46. [PubMed: 20177070]
20. Heller F, Fromm A, Gitter AH, Mankertz J, Schulzke JD. Epithelial apoptosis is a prominent feature of the epithelial barrier disturbance in intestinal inflammation: effect of pro-inflammatory interleukin-13 on epithelial cell function. Mucosal immunology. 2008; 1(Suppl 1):S58–61. [PubMed: 19079233]
21. Miossec P, van den Berg W. Th1/Th2 cytokine balance in arthritis. Arthritis and rheumatism. 1997; 40(12):2105–15. [PubMed: 9416846]
22. David M, Ford D, Bertoglio J, Maizel AL, Pierre J. Induction of the IL-13 receptor alpha2-chain by IL-4 and IL-13 in human keratinocytes: involvement of STAT6, ERK and p38 MAPK pathways. Oncogene. 2001; 20(46):6660–8. [PubMed: 11709700]
23. Donaldson DD, Whitters MJ, Fitz LJ, Neben TY, Finnerty H, Henderson SL, et al. The murine IL-13 receptor alpha 2: molecular cloning, characterization, and comparison with murine IL-13 receptor alpha 1. Journal of immunology (Baltimore, Md: 1950). 1998; 161(5):2317–24.
24. Mandal D, Fu P, Levine AD. REDOX regulation of IL-13 signaling in intestinal epithelial cells: usage of alternate pathways mediates distinct gene expression patterns. Cellular signalling. 2010; 22(10):1485–94. [PubMed: 20570727]
25. Wood N, Whitters MJ, Jacobson BA, Witek J, Sypek JP, Kasaian M, et al. Enhanced interleukin (IL)-13 responses in mice lacking IL-13 receptor alpha 2. The Journal of experimental medicine. 2003; 197(6):703–9. [PubMed: 12642602]
26. Hershey GK. IL-13 receptors and signaling pathways: an evolving web. The Journal of allergy and clinical immunology. 2003; 111(4):677–90. quiz 91. [PubMed: 12704343]
27. Kelly-Welch AE, Hanson EM, Boothby MR, Keegan AD. Interleukin-4 and interleukin-13 signaling connections maps. Science (New York, NY). 2003; 300(5625):1527–8.
28. Roy B, Bhattacharjee A, Xu B, Ford D, Maizel AL, Cathcart MK. IL-13 signal transduction in human monocytes: phosphorylation of receptor components, association with Jaks, and phosphorylation/activation of Stats. Journal of leukocyte biology. 2002; 72(3):580–9. [PubMed: 12223527]
29. Murata T, Husain SR, Mohri H, Puri RK. Two different IL-13 receptor chains are expressed in normal human skin fibroblasts, and IL-4 and IL-13 mediate signal transduction through a common pathway. International immunology. 1998; 10(8):1103–10. [PubMed: 9723696]
30. Atherton HC, Jones G, Danahay H. IL-13-induced changes in the goblet cell density of human bronchial epithelial cell cultures: MAP kinase and phosphatidylinositol 3-kinase regulation. American journal of physiology Lung cellular and molecular physiology. 2003; 285(3):L730–9. [PubMed: 12794003]
31. Iwashita J, Sato Y, Sugaya H, Takahashi N, Sasaki H, Abe T. mRNA of MUC2 is stimulated by IL-4, IL-13 or TNF-alpha through a mitogen-activated protein kinase pathway in human colon cancer cells. Immunology and cell biology. 2003; 81(4):275–82. [PubMed: 12848848]
32. Wright K, Kolios G, Westwick J, Ward SG. Cytokine-induced apoptosis in epithelial HT-29 cells is independent of nitric oxide formation. Evidence for an interleukin-13-driven phosphatidylinositol 3-kinase-dependent survival mechanism. The Journal of biological chemistry. 1999; 274(24): 17193–201. [PubMed: 10358077]
33. Rosen MJ, Frey MR, Washington MK, Chaturvedi R, Kuhnhein LA, Matta P, et al. STAT6 activation in ulcerative colitis: a new target for prevention of IL-13-induced colon epithelial cell dysfunction. Inflammatory bowel diseases. 2011; 17(11):2224–34. [PubMed: 21308881]
34. Zhang JG, Hilton DJ, Willson TA, McFarlane C, Roberts BA, Moritz RL, et al. Identification, purification, and characterization of a soluble interleukin (IL)-13-binding protein. Evidence that it is distinct from the cloned Il-13 receptor and Il-4 receptor alpha-chains. J Biol Chem. 1997; 272(14):9474–80. [PubMed: 9083087]

35. Daines MO, Tabata Y, Walker BA, Chen W, Warrier MR, Basu S, et al. Level of expression of IL-13R alpha 2 impacts receptor distribution and IL-13 signaling. Journal of immunology (Baltimore, Md: 1950). 2006; 176(12):7495–501.

36. Chen W, Sivaprasad U, Tabata Y, Gibson AM, Stier MT, Finkelman FD, et al. IL-13R alpha 2 membrane and soluble isoforms differ in humans and mice. Journal of immunology (Baltimore, Md: 1950). 2009; 183(12):7870–6.

37. Mentink-Kane MM, Cheever AW, Thompson RW, Hari DM, Kabatereine NB, Vennervald BJ, et al. IL-13 receptor alpha 2 down-modulates granulomatous inflammation and prolongs host survival in schistosomiasis. Proceedings of the National Academy of Sciences of the United States of America. 2004; 101(2):586–90. [PubMed: 14699044]

38. Fichtner-Feigl S, Strober W, Kawakami K, Puri RK, Kitani A. IL-13 signaling through the IL-13alpha2 receptor is involved in induction of TGF-beta1 production and fibrosis. Nature medicine. 2006; 12(1):99–106.

39. Fujisawa T, Joshi BH, Puri RK. IL-13 regulates cancer invasion and metastasis through IL-13Ralpha2 via ERK/AP-1 pathway in mouse model of human ovarian cancer. International journal of cancer Journal international du cancer. 2012; 131(2):344–56. [PubMed: 21858811]

40. Rahaman SO, Vogelbaum MA, Haque SJ. Aberrant Stat3 signaling by interleukin-4 in malignant glioma cells: involvement of IL-13Ralpha2. Cancer research. 2005; 65(7):2956–63. [PubMed: 15805299]

41. Barderas R, Bartolome RA, Fernandez-Acenero MJ, Torres S, Casal JI. High expression of IL-13 receptor alpha2 in colorectal cancer is associated with invasion, liver metastasis, and poor prognosis. Cancer research. 2012; 72(11):2780–90. [PubMed: 22505647]

42. Zeissig S, Bojarski C, Buergel N, Mankertz J, Zeitz M, Fromm M, et al. Downregulation of epithelial apoptosis and barrier repair in active Crohn's disease by tumour necrosis factor alpha antibody treatment. Gut. 2004; 53(9):1295–302. [PubMed: 15306588]

43. Olsen J, Gerds TA, Seidelin JB, Csillag C, Bjerrum JT, Troelsen JT, et al. Diagnosis of ulcerative colitis before onset of inflammation by multivariate modeling of genome-wide gene expression data. Inflammatory bowel diseases. 2009; 15(7):1032–8. [PubMed: 19177426]

44. Edgar R, Domrachev M, Lash AE. Gene Expression Omnibus: NCBI gene expression and hybridization array data repository. Nucleic acids research. 2002; 30(1):207–10. [PubMed: 11752295]

45. Moehle C, Ackermann N, Langmann T, Aslanidis C, Kel A, Kel-Margoulis O, et al. Aberrant intestinal expression and allelic variants of mucin genes associated with inflammatory bowel disease. Journal of molecular medicine (Berlin, Germany). 2006; 84(12):1055–66.

46. Zeissig S, Bürgel N, Günzel D, Richter J, Mankertz J, Wahnschaffe U, et al. Changes in expression and distribution of claudin 2, 5 and 8 lead to discontinuous tight junctions and barrier dysfunction in active Crohn's disease. Gut. 2007; 56(1):61–72. [PubMed: 16822808]

47. Dames P, Bergann T, Fromm A, Bucker R, Barmeyer C, Krug SM, et al. Interleukin-13 affects the epithelial sodium channel in the intestine by coordinated modulation of STAT6 and p38 MAPK activity. The Journal of physiology. 2015

48. Turner JR. Intestinal mucosal barrier function in health and disease. Nature reviews Immunology. 2009; 9(11):799–809.

49. Richter JF, Schmauder R, Krug SM, Gebert A, Schumann M. A novel method for imaging sites of paracellular passage of macromolecules in epithelial sheets. Journal of controlled release: official journal of the Controlled Release Society. 2016; 229:70–9. [PubMed: 26995760]

50. Kolosov D, Kelly SP. A role for tricellulin in the regulation of gill epithelium permeability. American journal of physiology Regulatory, integrative and comparative physiology. 2013; 304(12):R1139–48.

51. Ahmad R, Chaturvedi R, Olivares-Villagomez D, Habib T, Asim M, Shivesh P, et al. Targeted colonic claudin-2 expression renders resistance to epithelial injury, induces immune suppression, and protects from colitis. Mucosal immunology. 2014; 7(6):1340–53. [PubMed: 24670427]

52. Keely S, Feighery L, Campion DP, O'Brien L, Brayden DJ, Baird AW. Chloride-led disruption of the intestinal mucous layer impedes Salmonella invasion: evidence for an 'enteric tear'

mechanism. Cellular physiology and biochemistry: international journal of experimental cellular physiology, biochemistry, and pharmacology. 2011; 28(4):743–52.

53. Reinisch W, Panes J, Khurana S, Toth G, Hua F, Comer GM, et al. Anrukinzumab, an anti-interleukin 13 monoclonal antibody, in active UC: efficacy and safety from a phase IIa randomised multicentre study. Gut. 2015; 64(6):894–900. [PubMed: 25567115]
54. Danese S, Rudzinski J, Brandt W, Dupas JL, Peyrin-Biroulet L, Bouhnik Y, et al. Tralokinumab for moderate-to-severe UC: a randomised, double-blind, placebo-controlled, phase IIa study. Gut. 2015; 64(2):243–9. [PubMed: 25304132]
55. De Boever EH, Ashman C, Cahn AP, Locantore NW, Overend P, Pouliquen IJ, et al. Efficacy and safety of an anti-IL-13 mAb in patients with severe asthma: a randomized trial. The Journal of allergy and clinical immunology. 2014; 133(4):989–96. [PubMed: 24582316]
56. Hodsman P, Ashman C, Cahn A, De Boever E, Locantore N, Serone A, et al. A phase 1, randomized, placebo-controlled, dose-escalation study of an anti-IL-13 monoclonal antibody in healthy subjects and mild asthmatics. British journal of clinical pharmacology. 2013; 75(1):118–28. [PubMed: 22616628]
57. Kreusel KM, Fromm M, Schulzke JD, Hegel U. Cl-secretion in epithelial monolayers of mucus-forming human colon cells (HT-29/B6). The American journal of physiology. 1991; 261(4 Pt 1):C574–82. [PubMed: 1656765]
58. Stockmann M, Gitter AH, Sorgenfrei D, Fromm M, Schulzke JD. Low edge damage container insert that adjusts intestinal forceps biopsies into Ussing chamber systems. Pflugers Archiv: European journal of physiology. 1999; 438(1):107–12. [PubMed: 10370094]

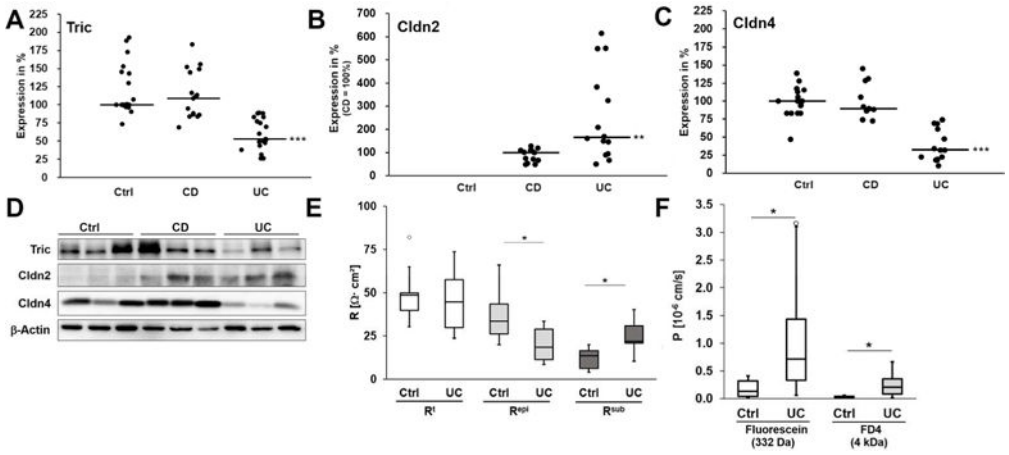

Fig. 1. Expression, functional and electrophysiological analysis of human biopsies

A. Scatterplot of tricellulin protein expression in sigmoid colon biopsies of Ctrl, CD and UC. Median of Ctrl is set 100%. Tricellulin is downregulated in UC, while in CD no difference to controls occurs (median; Ctrl: 100.0%, n=20; CD: 108.6%, n=17; UC: 53.0%, n=19, ***p<0.001). **B.** Scatterplot of claudin-2 protein expression in sigmoid colon of Ctrl, CD and UC. Because Ctrl patients show no claudin-2 expression, the median of CD is set 100%. In both diseases claudin-2 is upregulated, however in UC this increase is higher than in CD (**p<0.01). **C.** Scatterplot of claudin-4 protein expression in sigmoid colon of Ctrl, CD and UC. Median of Ctrl is set 100%. Claudin-4 is downregulated in UC, while in CD no significant difference to Ctrl occurs (Ctrl: 100.0%, n=15; CD: 89.4%, n=11; UC: 32.3%, n=13, ***p<0.001). **D.** Representative western blot images of sigmoid colon tissue of Ctrl, CD and UC. **E.** Electrical resistances of sigmoid colon of Ctrl and UC (n=8). While the epithelial resistance (R^{epi}) is decreased in UC (*p<0.05), the resistance of the subepithelial layers (R^{sub}) is increased (*p<0.05), resulting in an almost unchanged transepithelial resistance (R^{t}). **F.** Permeability for the paracellular flux markers fluorescein and 4 kDa-FITC dextran. Both permeabilities are increased in UC (fluorescein: Ctrl: $0.18\pm0.07\cdot10^{-6}$ cm/s, n=6, UC: $1.07\pm0.41\cdot10^{-6}$ cm/s, n=7, *p<0.05; FD4: Ctrl: $0.03\pm0.01\cdot10^{-6}$ cm/s, n=6, UC: $0.26 \pm 0.10\cdot10^{-6}$ cm/s, n=6, *p<0.05).

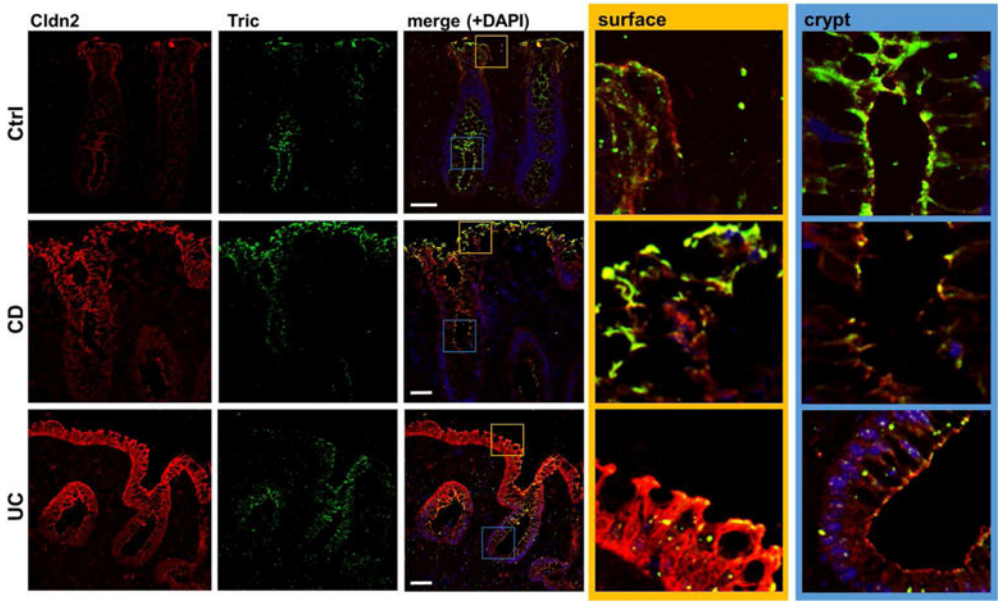

Fig. 2. Localization of claudin 2 (red) and tricellulin (green) in human colon biopsies

Representative immunofluorescent stainings of cryosections of patient biopsies. While claudin-2 is only expressed within the crypts of control patients (ctrl), it is expressed all along the crypt and surface in CD and UC patients. Tricellulin is present in all areas of the crypt and is also detectable in surface areas of the control patients. In UC, a decreased expression is observed, while in CD patients there seems to be a shift of expression; while in the crypts the signal appears to be reduced, localization within the surface is increased. The merged localizations within the crypt (blue box) and the surface epithelium (yellow) are also shown in higher magnifications. Bar = 50 nm.

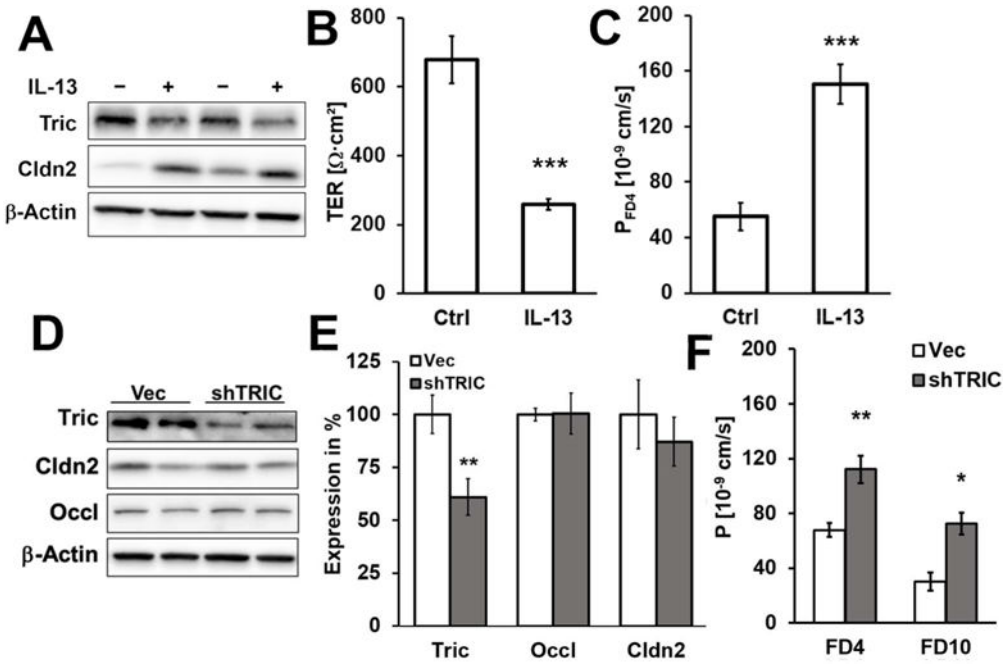

Fig. 3. Expression and functional analysis of intestinal cells

A. Representative western blots. IL-13 treatment lead to decreased tricellulin (72±4%,***p<0.001;n=11) and increased claudin-2 (145±14%,**p>0.01;n=7) expression in HT-29/B6 (densitometry Fig. 4E). **B.** Effect of IL-13 on transepithelial resistance. 48 h incubation with IL-13 decreases R^t in HT-29/B6 (***p<0.001). **C.** Effect of IL-13 on permeability for 4 kDa-FITC dextran (FD4). 48 h incubation with IL-13 increases permeability to FD4 in HT-29/B6 (***p<0.001) **D.** Representative western blots. **E.** Densitometric analysis of protein expression levels in stable shTRIC transfectants in comparison to vector-transfected controls. shTRIC leads to decreased tricellulin expression (60±9%, **p<0.01, n=10), but had no influence on expression of claudin-2 (87±12%, n=5) or occludin (Occl; 100±10%, n=5). **F.** Permeability for the macromolecular paracellular fluxmarkers 4 kDa-and 10 kDa-FITC dextran. Both permeabilities are increased in shTRIC clones (FD4: **p<0.01; FD10: *p<0.05).

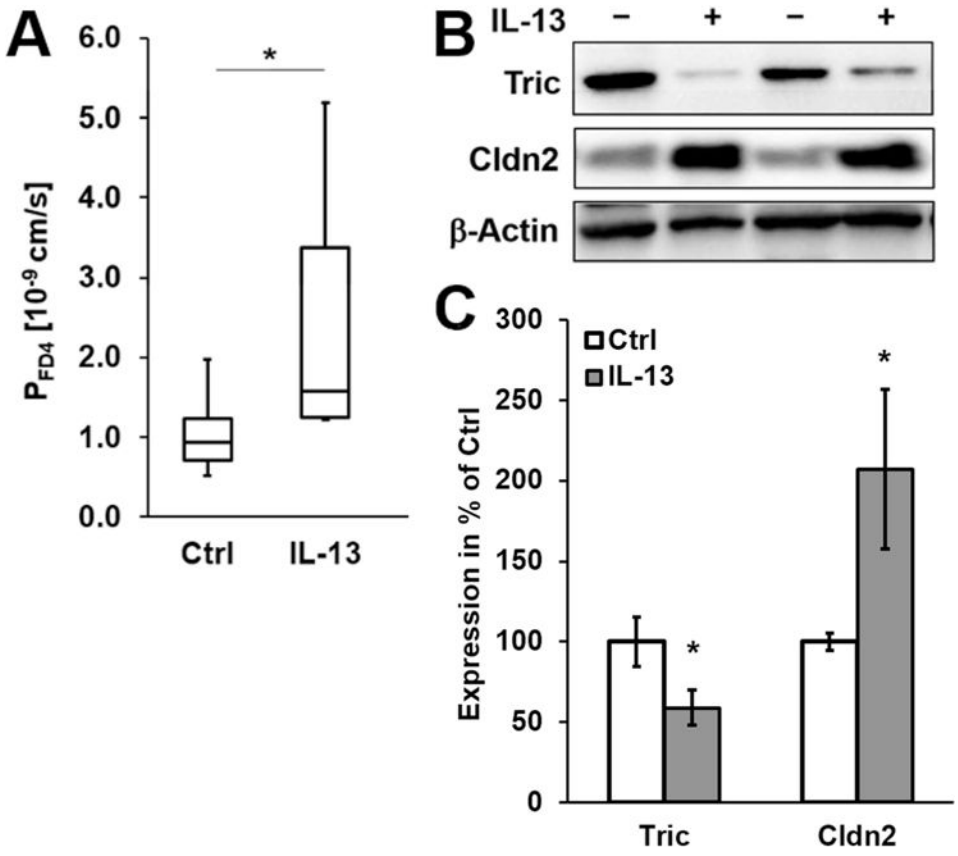

Fig. 4. Functional and expression analysis of mice treated with IL 13

A. Permeability for 4 kDa-FITC dextran. Permeability for FD4 is increased in mice treated with IL-13 (*$p<0.05$, n=9–12). **B.** Representative western blots. Treatment of mice with IL-13 results in increased claudin-2 and decreased tricellulin expression. **C.** Densitometric analysis of protein expression colon tissue of untreated and IL-13-treated mice. After treatment, claudin-2 is increased and tricellulin is decreased (*$p<0.05$, n=9–12).

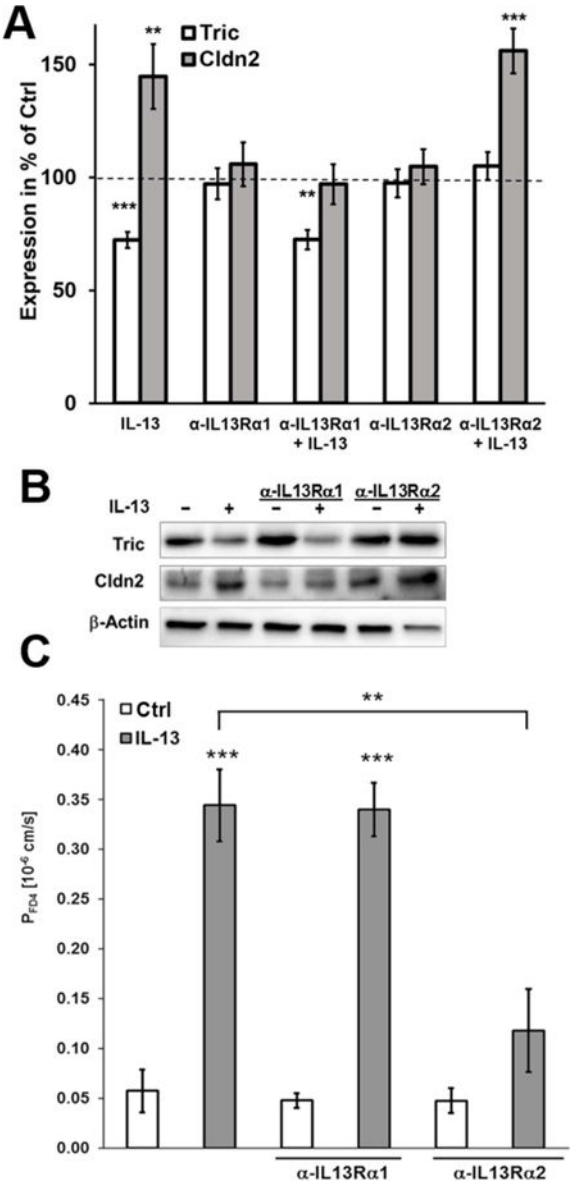

Fig. 5. Analysis of the involvement of IL13 receptors in regulation of tricellulin and claudin 2

A. Densitometric analysis of protein expression of HT-29/B6 cells treated with inhibitory antibodies and IL-13. In HT-29/B6, the inhibitory antibody against IL13 receptor α1 is able to inhibit the IL-13-caused increase of claudin-2, but not the decrease of tricellulin. Tricellulin decrease by IL-13 is inhibited by blocking the IL-13 receptor α 2, while its inhibition has no effect on the claudin-2 increase (n=7–11). **B.** Representative western blots of the incubation with inhibitory antibodies and IL-13. **C.** Permeability for 4 kDa-FITC dextran. Permeability for FD4 is increased in HT-29/B6 cells treated with IL-13. This effect was not inhibited by preincubation with the inhibitory antibody against IL13 receptor α1, but was abolished by preincubation with the inhibitory antibody against IL13 receptor α2 (**p<0.01; ***p<0.001, n=4).

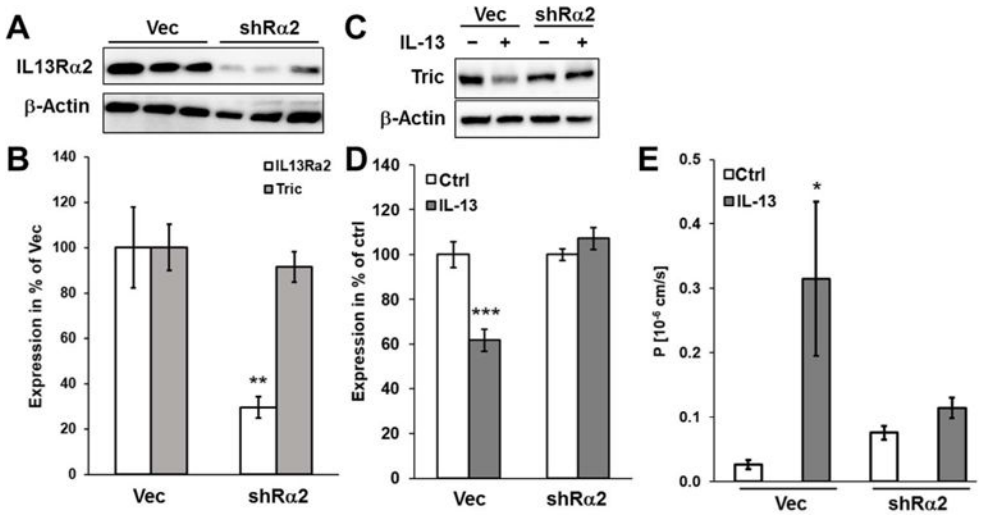

Fig. 6. Effects of IL13Rα2 knockdown

A. Representative western blots of different clones of HT-29/B6 cells stably transfected with shRNA against IL13Rα2 (shRα2) in comparison with vector-transfected controls. **B.** Densitometric analysis of tricellulin and IL13Rα2 expression in shRα2 knockdown clones (n=4; **p<0.01). **C.** Representative western blots of vector controls and shRα2 clones treated with IL-13. **D.** Densitometric analysis of tricellulin expression in shRα2 and vector control clones in response to IL-13-treatment (n=6; ***p<0.001). **E.** Permeability for 4 kDa-FITC dextran. Permeability for FD4 is increased in vector controls treated with IL-13, while in IL13Rα2 knockdown, no effect is observed after IL-13 treatment (n=8–13; *p<0.05).

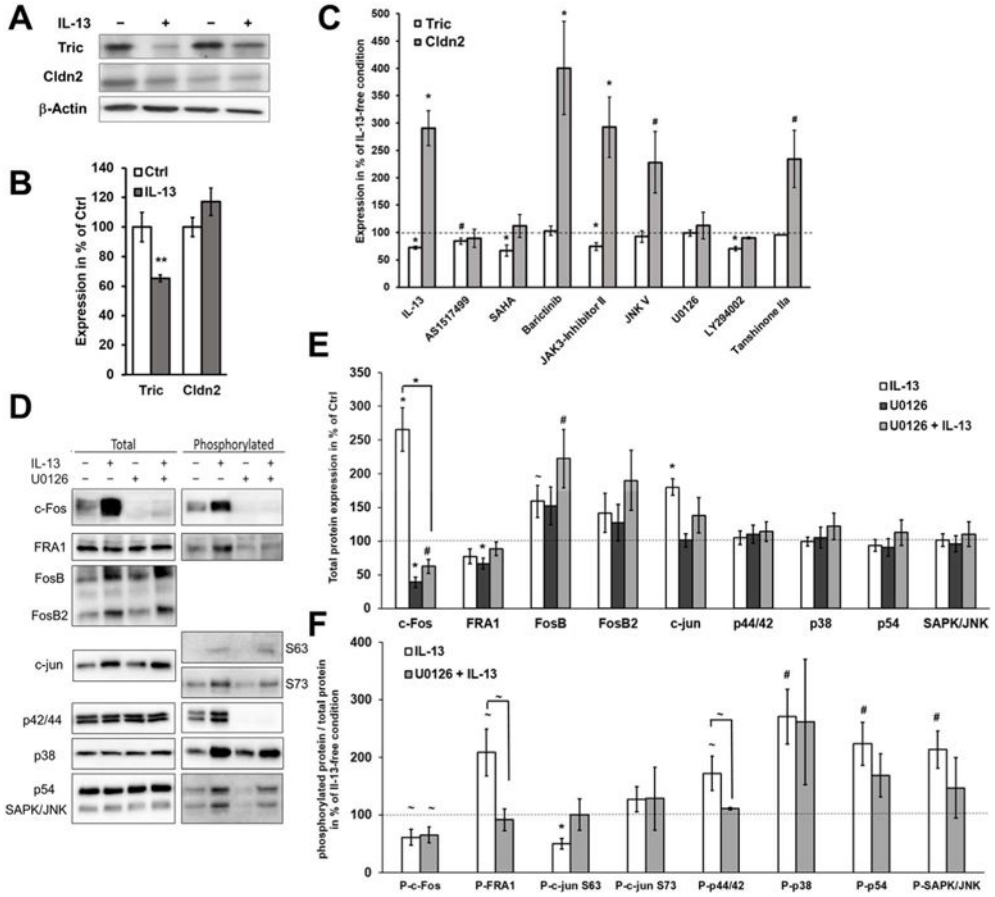

Fig. 7. Analysis of the signaling pathways regulating tricellulin and claudin 2

A. Representative western blots of STAT6$^{-/-}$ mice treated with IL-13. IL-13 treatment still decreases tricellulin, while claudin-2 expression is at levels of untreated mice due to absence of STAT6 (n=4–6). **B.** Densitometric analysis of protein expression in colon tissue of untreated and IL-13-treated STAT6$^{-/-}$ mice. After treatment, tricellulin is decreased (**p<0.01), while claudin-2 is unaffected. **C.** Densitometric analysis of protein expression of HT-29/B6 pretreated with different inhibitors before application of IL-13 (representative blots see Fig. S6, n=4–12). Protein expression levels were normalized to the respective inhibitor treatment without IL-13. Inhibitors targeting STAT6, ERK1/2, MAPK, and PI3K affect the IL-13-caused increase of claudin-2, while inhibitors targeting JAK1 and/or JAK2, JNK, ERK1/2, MAPK and AP-1 inhibit the IL-13-caused decrease of tricellulin (#p<0.05; *p<0.01, n=6–12). **D.** Representative western blots of total and phosphorylated proteins involved in ERK1/2 and AP-1 signaling. HT-29/B6 cells are either pretreated or not with U0126 before application of IL-13. **E.** Densitometric analysis of total protein. Expression of cFos, FosB and c-jun is increased by IL-13 (*p<0.001, #p<0.01, ~p<0.05; n=12). U0126 inhibits this increase for c-Fos (IL-13: 265±33%, ***p<0.001; U0126+IL-13: 63±11 %, ***p<0.001 to IL-13). **F.** Ratio of phosphorylated protein to total protein under influence of IL-13. Phosphorylation levels are increased by IL-13 for FRA-1, p44/42, p38, p54 and SAPK/JNK and decreased for c-Fos and c-jun (S63; IL-13: 50±10%, ***p<0.001; U0126+IL-13: 92±18 %, *p<0.05 to IL-13, n=12). These changes in phosphorylation are

inhibited by U0126 only for FRA-1 (IL-13: 209±41%, *p<0.05; U0126 + IL-13: 92±19 %, *p<0.05 to IL-13, n=12) and p44/42 (ERK1/2; IL-13: 173±30%, *p<0.05; U0126+IL-13: 6±2 %, *p<0.05 to IL-13, n=12) (n=10–12).

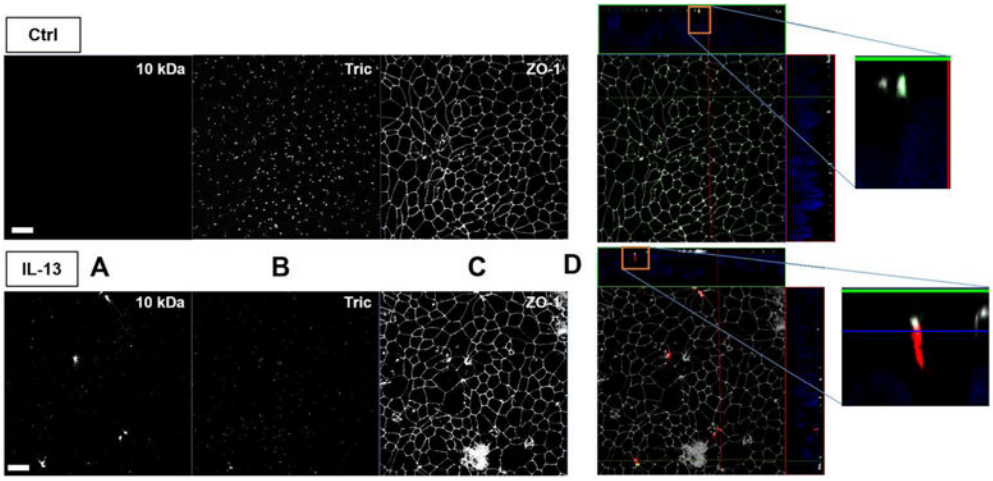

Fig. 8. Visualization of macromolecule passage sites by sandwich assay

Maximum intensity projections and Z-stacks of HT-29/B6 immunofluorescence stainings. One out of four experiments is shown here, all yielding the same result. Cells were either untreated (upper panel) or treated with IL-13 (lower panel) and incubated basolaterally with avidin and then apically with biotin- and TRITC-labelled 10 kDa-dextran (**A**). Tricellulin (**B**) and ZO-1 (**C**) were counterstained for localization of the macromolecular passage. In merged views featuring Z-stacks and enlarged Z-stacks (**D**), 10 kDa dextran is shown in red, tricellulin in green, and ZO-1 in gray. IL-13 treatment results in decrease of tricellulin, while 10 kDa dextran appears predominantly at sites where more than two cells are in contact. For clearer evaluation of the localization of tricellulin, its signals were increased in contrast, while the ZO-1 signals were decreased in D. Bar = 20 μm.

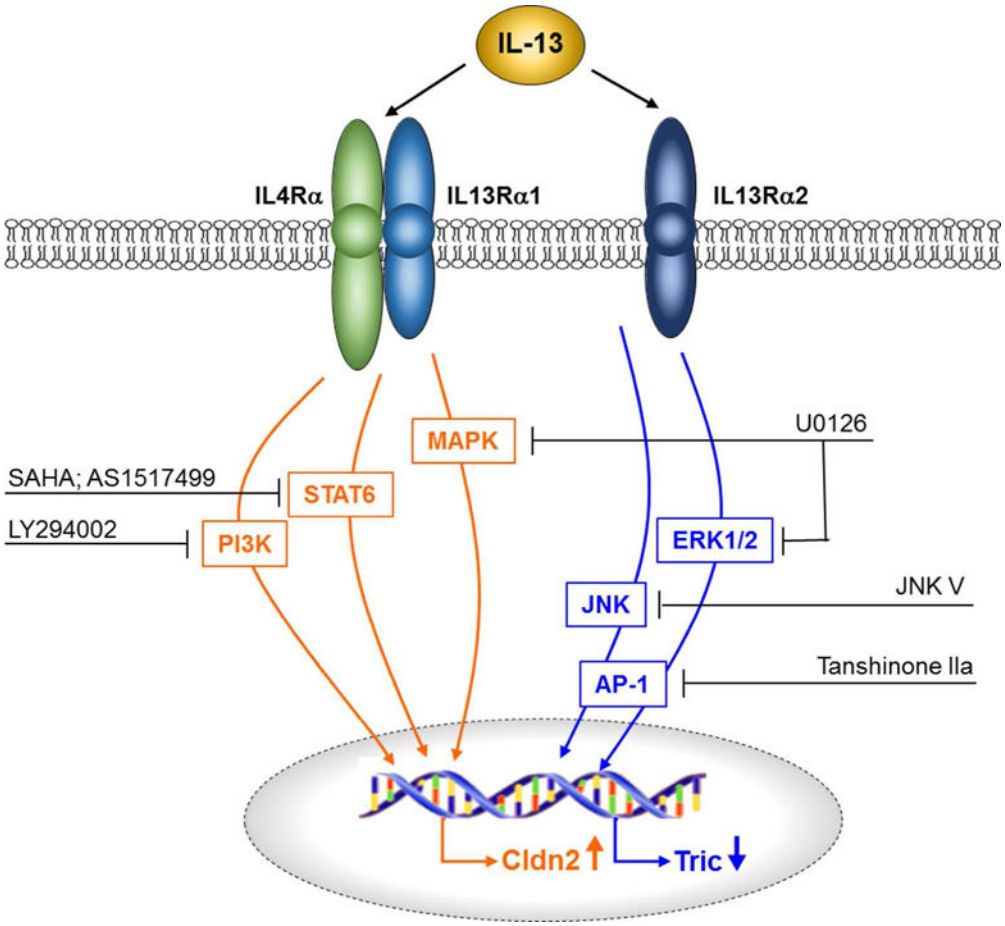

Fig. 9. Schematic view of signaling pathways for claudin 2 and tricellulin triggered by IL 13

While claudin-2 expression is regulated via interaction of IL-13 with the IL4Rα/IL13Rα1 complex, tricellulin expression is regulated via interaction of IL-13 with IL13Rα2 and the downstream signaling cascades.

Table. 1

Cytokine and inhibitor experiments

cytokine	concentration	source
TNFα	500 U/mL	Peprotech, Hamburg, Germany
IL-4	100 ng/mL	Peprotech, Hamburg, Germany
INFγ	50 U/mL	Peprotech, Hamburg, Germany
TGFβ1	10 ng/mL	Peprotech, Hamburg, Germany
TGFβ2	10 ng/mL	Peprotech, Hamburg, Germany
IL-13	100 ng/mL	Peprotech, Hamburg, Germany

inhibitor	concentration	source
SAHA	5 μM	Sigma-Aldrich, Schnelldorf, Germany
Tanshinone Iia	10 μM	Sigma-Aldrich, Schnelldorf, Germany
LY294002	10 μM	Calbiochem, Darmstadt, Germany
JAK3-Inhibitor II	50 μM	Calbiochem, Darmstadt, Germany
JNK V	10 μM	Calbiochem, Darmstadt, Germany
U0126	10 μM	Cell Signaling Technology, Frankfurt am Main, Germany
AS151-499	1 μg/mL	Axon Medchem, Groningen, Netherlands
Baricitinib	250 nM	Selleckchem, Munich, Germany